



# Improving the MPC Performance of the Model in Order to Improve the Frequency Stability of the Two-Area Microgrid

 Farhad Amiri<sup>1</sup> |  Mohammad Hassan Moradi<sup>2</sup>

Department of Electrical Engineering, Faculty of Engineering, Bu-Ali Sina University.<sup>1,2</sup>  
Corresponding author's email: [mhmoradi@basu.ac.ir](mailto:mhmoradi@basu.ac.ir)

Article Info	ABSTRACT
<b>Article type:</b> Research Article	<p>In the context of frequency stability in a two-area microgrid, it is crucial to address the fluctuations in frequency caused by load disturbances. To achieve this, an effective load-frequency control (LFC) system, which serves as the secondary control, must be implemented. However, the presence of renewable energy sources such as wind turbines and photovoltaic systems adds complexity to the operation of the LFC system due to their inherent uncertainty. To enhance the performance of the LFC system in the two-area microgrid, this paper proposes a reduction in the number of controllers employed, aiming for a less complex structure. Specifically, Model Predictive Control (MPC) is utilized for LFC, and the weight parameters of the MPC controller are determined using Craziness-based Particle Swarm Optimization (CRPSO). The proposed method is compared with alternative approaches, including PID controller optimized with Social Spider Optimization (SSO), Fractional Order Fuzzy PI (FOFPI), and conventional MPC. The effectiveness of the proposed method is evaluated in various scenarios, considering load variations and the presence of distributed microgrid generation resources. The results demonstrate that the proposed method outperforms the other controllers in terms of speed of response, reduction of overshoot and undershoot, and overall complexity. Importantly, the proposed method significantly improves the frequency stability of the two-area microgrid. The simulation and analysis are conducted using MATLAB software, providing a comprehensive understanding of the system dynamics and the performance of the proposed controller.</p>
<b>Article history:</b> Received: 11-December-2023 Received in revised form: 12-March-2024 Accepted: 23-April-2024 Published online: 22-Sep-2024	
<b>Keywords</b> Less complexity, Social Spider Optimization, Model Predictive Control, Craziness-based Particle Swarm Optimization.	

## I. Introduction

The increasing adoption of renewable energy sources in the electricity industry has led to a rise in the deployment of microgrids, which are small power networks operating at medium voltage levels. These microgrids incorporate a combination of renewable energy sources, traditional energy sources, energy storage systems, and localized loads [1]. Microgrids can operate in either grid-connected or islanded mode, providing flexibility and resilience to the power system. Additionally, interconnections between microgrids in a geographical area enable the formation of multi-area

microgrids, such as the two-area microgrid configuration. One of the challenges associated with integrating renewable energy sources into microgrids is their inherent variability due to the unpredictable nature of wind and solar radiation. Fluctuations in the power output of renewable sources, coupled with changes in load demand, can lead to imbalances and significant deviations in the microgrid frequency when operating in islanded mode [2]. To address this issue, Load-Frequency Control (LFC) strategies are employed to mitigate power and frequency fluctuations, restore the frequency to its nominal value, and maintain power exchange between interconnected microgrids [1-3].

Wind turbines and photovoltaic systems are significant contributors to distributed production within microgrids. While these renewable energy sources offer numerous advantages, they also present challenges for microgrid control [4]. The variable nature of power production from wind turbines and photovoltaic systems introduces fluctuations in the microgrid's overall power supply. These fluctuations, combined with load disturbances, can disrupt the balance within the islanded microgrid, resulting in substantial frequency deviations [2].

To address these challenges, Load-Frequency Control (LFC) strategies are utilized. These strategies aim to mitigate power and frequency fluctuations, restore the frequency to its nominal value, and maintain power flow across communication lines within the microgrid [1-3]. The frequency control strategy in an islanded microgrid typically employs two control loops: the primary control loop and the secondary control loop. The primary control loop plays a crucial role in limiting frequency deviations following a disturbance. However, it is unable to restore the frequency to its nominal value. Hence, a secondary control loop, known as secondary frequency control, is employed to restore the frequency to its desired set point [4-6]. While the primary control loop is typically implemented on the diesel generator, the secondary control loop requires different controllers to manage the LFC system. The performance of the controllers used within the secondary control loop is of utmost importance to ensure effective frequency control in the microgrid [4-6]. These controllers are responsible for regulating power generation or consumption within the microgrid, enabling the restoration of frequency to its nominal value. The selection and design of appropriate controllers are critical factors in achieving accurate and efficient frequency regulation.

Extensive research has been done in connection with LFC in microgrids. LFC methods in microgrids can be divided into two general categories. 1) Islanded microgrid [7-27]. Two-area microgrid [28-30].

Several controllers such as conventional PI [7, 8], conventional PID [9], PID based on coefficient determination by Ziegler-Nichols method [10], PID based on GA [11], PI based on PSO [12] PID based on BIO [13], PI/PID based on QOH [14], PID based on fractional order [15], fuzzy-PID based on fractional order [16], PI based on type 2-fuzzy logic in combination with improved HSA [17, 18], fuzzy-PID based on PSO [19], PID based on HBEL [20] for LFC Presented in microgrids. PID controller is a common controller in LFC systems related to microgrids. However, this controller also has problems, such as that it does not perform well against the disturbances on the microgrid, and it does not have the ability to weaken these disturbances, and it also does not perform well against the uncertainty of the parameters related to the islanded microgrid.

The robust controller based on the  $H_\infty$  has been used to

control the LFC related to the microgrid [21-23]. One of the main problems of the robust controller ( $H_\infty$ ) in the LFC system is that it requires accurate information about the disturbances and uncertainty of the system parameters, which greatly increases the complexity of the design of this controller.

In [24], the self-adjusting order fuzzy controller has been used to control the load frequency related to the islanded microgrid. In [25], coordinated control of electric vehicles and renewable energy sources is used for frequency control in microgrids. In [26, 27], a robust control method has been presented to improve frequency stability in the power system with the presence of a wind turbine. The presence of the wind turbine causes more uncertainty and disturbance in the power system and ultimately complicates the load-frequency control problem.

The issue of LFC in a two-area microgrid is of significant importance. The LFC system not only focuses on regulating the frequency within each microgrid but also plays a crucial role in controlling the power fluctuations between the interconnected microgrids [28-30].

In [28], the effect of time delay of telecommunication systems on the stability of LFC in a system consisting of a two-area microgrid has been investigated. The presence of time delay will cause problems in the LFC function and endanger the frequency stability of the two-area microgrid. In [29], a tertiary monitoring control strategy for LFC in a two-area microgrid is presented. In [30], the LFC in a two-area microgrid with the PID method optimized with SSO is presented.

In the existing methods [7-30], energy storage sources are often treated as uncontrollable sources, or separate controllers are employed to manage energy storage devices such as batteries, flywheels, and superconducting storage systems. These approaches introduce additional complexity by increasing the number of microgrid controllers. Moreover, when it comes to Load-Frequency Control (LFC) in a two-area microgrid, these methods exhibit limitations in effectively addressing system disturbances and uncertainties in system parameters. Consequently, there is a pressing need for a suitable control method that can robustly handle such issues. MPC is a widely utilized controller in the industry that offers promising solutions. Unlike conventional methods, MPC demonstrates resilience in the face of system disturbances and uncertainties in parameters. This control methodology incorporates the ability to predict future events, enabling proactive decision-making and response. By leveraging predictive capabilities, MPC can anticipate changes in power generation, load demand, and other system dynamics, thereby facilitating effective frequency regulation and power balance in the microgrid.

One of the most important factors related to the MPC of the model is the weight parameters, whose optimal setting makes the MPC play an effective role against the disturbances and

uncertainty of the two-area microgrid parameters.

Therefore, in this paper, the CRPSO has been used to adjust the weight parameters of the MPC in the two-area microgrid. CRPSO has many advantages over other optimization algorithms, including [31-34]:

The (CRPSO) algorithm offers several advantages over other optimization algorithms:

- **Enhanced Exploration:** CRPSO introduces a higher level of randomness and exploration compared to other algorithms. This allows CRPSO to effectively explore a larger search space, potentially discovering better solutions that may be missed by other algorithms that rely on more deterministic search strategies.
- **Population-Based Approach:** CRPSO operates on a population of particles that communicate and cooperate with each other. This population-based approach enables information sharing and collective intelligence, leading to faster convergence and improved global search capabilities.
- **Flexibility and Adaptability:** CRPSO is highly flexible and adaptable to different problem domains. It can handle both continuous and discrete optimization problems, making it applicable to a wide range of real-world scenarios. Additionally, CRPSO can easily incorporate problem-specific constraints and objectives, making it a versatile algorithm for various optimization tasks.
- **Efficient Convergence:** CRPSO tends to converge to optimal or near-optimal solutions relatively quickly. The collective learning and sharing of information among particles allow the algorithm to exploit promising regions of the search space efficiently, leading to faster convergence and better overall performance.
- **Easy Implementation and Parameter Tuning:** CRPSO is relatively easy to implement and does not require
- complex operators or encoding schemes. It has a small number of intuitive parameters that can be tuned to adapt to specific problem characteristics, making it accessible to both researchers and practitioners.

It's important to note that the effectiveness of CRPSO, like any optimization algorithm, can vary depending on the

problem being addressed. Therefore, it is essential to carefully analyze the problem requirements and consider the specific characteristics and limitations of CRPSO before applying it. In general, the innovations of this paper include the following sections:

- 1) Reduction of controllers used for energy storage systems such as batteries, flywheels and SMES (less complexity).
- 2) LFC in two-area microgrid based on MPC.
- 3) Improving the performance and adjusting the weight parameters related to the MPC against disturbances and uncertainty related to the two-area microgrid parameters using the CRPSO.
- 4) Testing the performance of the proposed algorithm compared to GA and PSO algorithms in optimizing the weight parameters of the MPC considering the ITAE objective function.
- 5) Performance testing of the proposed controller (MPC(CRPSO)) in order to improve the performance of LFC against disturbances and uncertainty of the parameters related to the two-area microgrid.

The paper consists of several sections. In the second part, the model and components of the studied two-area microgrids have been discussed, in the third part, the state space equations of the two-area microgrid have been discussed, in the fourth part, the design of the proposed controller for the two-area microgrid has been discussed, and in the fifth part, the simulation has been described. And the results.

## **II. The model and components of the studied two-area microgrid:**

### *A. Two-area microgrid model*

Fig. 1 illustrates the block diagram of a two-area microgrid, where the microgrid of the first area is connected to the microgrid of the second area through a communication line. The microgrid of the first area comprises a WTG, a DEG<sub>1</sub>, and SMES system. On the other hand, the microgrid of the second area consists of a DEG<sub>2</sub>, PV panels, and BESS. The primary source of power supply in the microgrid is the wind turbines, which are operated at their MPPT to maximize energy extraction. However, due to the variable nature of wind power output, the DEG<sub>1</sub> serves as a backup power source to meet load demand during periods of low wind power generation. The DEG<sub>1</sub> dynamically adjusts its power output to respond to changes in load requirements [28-30].

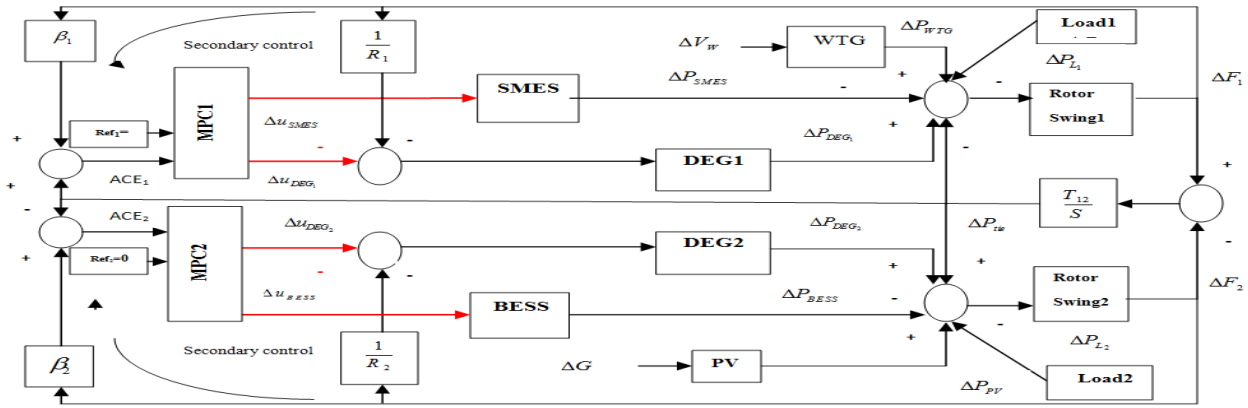


Fig. 1. The block diagram of the two-area microgrid [25, 27]

### III. The state-space equations of the two-area microgrid

#### A. The state space equations related to the microgrid of the first region

Due to the fact that the components of the microgrid are different in each region, therefore, each MPC has different state-space equations in each region. Therefore, the state-space equation of the microgrid of the first region are according to Equation (1).

$$\begin{bmatrix} \dot{\Delta F}_1 \\ \dot{\Delta P}_{DEG1} \\ \dot{\Delta X}_{s1} \\ \dot{\Delta P}_{SMES} \\ \dot{\Delta P}_{ac} \end{bmatrix} = \begin{bmatrix} -\frac{1}{T_{p1}} & \frac{k_{p1}}{T_{p1}} & 0 & -\frac{k_{p1}}{T_{p1}} & -\frac{k_{p1}}{T_{p1}} \\ 0 & -\frac{1}{T_{e1}} & \frac{k_{e1}}{T_{e1}} & 0 & 0 \\ -\frac{1}{R_1 T_{v1}} & 0 & -\frac{1}{T_{v1}} & 0 & 0 \\ 0 & 0 & 0 & -\frac{1}{T_L} & 0 \\ T_{i2} & 0 & 0 & 0 & 0 \end{bmatrix} \begin{bmatrix} \Delta F_1 \\ \Delta P_{DEG1} \\ \Delta X_{s1} \\ \Delta P_{SMES} \\ \Delta P_{ac} \end{bmatrix} + \begin{bmatrix} 0 & 0 \\ 0 & 0 \\ -\frac{1}{T_{v1}} & 0 \\ 0 & \frac{k_L}{T_L} \\ 0 & 0 \end{bmatrix} \begin{bmatrix} \Delta u_{DEG1} \\ \Delta u_{SMES} \end{bmatrix} + \begin{bmatrix} -\frac{k_{p1}}{T_{p1}} & \frac{k_{p1}}{T_{p1}} & 0 \\ 0 & 0 & 0 \\ 0 & 0 & 0 \\ 0 & 0 & -T_{i2} \end{bmatrix} \begin{bmatrix} \Delta P_{L1} \\ \Delta P_{WTG} \\ \Delta F_2 \end{bmatrix} \quad (1)$$

$$y = ACE_1 = [B_1 \ 0 \ 0 \ 0 \ 0 \ 1] \begin{bmatrix} \Delta F_1 \\ \Delta P_{DEG1} \\ \Delta X_{s1} \\ \Delta P_{SMES} \\ \Delta P_{ac} \end{bmatrix}$$

#### B. The state space equations related to the microgrid of the second region

Based on Fig. 1, the state-space equation related to the microgrid of the second region have been obtained according to Equation (2).

$$\begin{bmatrix} \dot{\Delta F}_2 \\ \dot{\Delta P}_{DEG2} \\ \dot{\Delta X}_{s2} \\ \dot{\Delta P}_{BESS} \\ \dot{\Delta P}_{ac} \end{bmatrix} = \begin{bmatrix} -\frac{1}{T_{p2}} & \frac{k_{p2}}{T_{p2}} & 0 & -\frac{k_{p2}}{T_{p2}} & \frac{k_{p2}}{T_{p2}} \\ 0 & -\frac{1}{T_{e2}} & \frac{k_{e2}}{T_{e2}} & 0 & 0 \\ -\frac{1}{R_2 T_{v2}} & 0 & -\frac{1}{T_{v2}} & 0 & 0 \\ 0 & 0 & 0 & -\frac{1}{T_8} & 0 \\ -T_{i2} & 0 & 0 & 0 & 0 \end{bmatrix} \begin{bmatrix} \Delta F_2 \\ \Delta P_{DEG2} \\ \Delta X_{s2} \\ \Delta P_{BESS} \\ \Delta P_{ac} \end{bmatrix} + \begin{bmatrix} 0 & 0 \\ 0 & 0 \\ -\frac{1}{T_{v2}} & 0 \\ 0 & \frac{k_{BESS}}{T_{BESS}} \\ 0 & 0 \end{bmatrix} \begin{bmatrix} \Delta u_{DEG2} \\ \Delta u_{BESS} \end{bmatrix} + \begin{bmatrix} \frac{k_{p2}}{T_{p2}} & \frac{k_{p2}}{T_{p2}} & 0 \\ 0 & 0 & 0 \\ 0 & 0 & 0 \\ 0 & 0 & 0 \\ 0 & 0 & -T_{i2} \end{bmatrix} \begin{bmatrix} \Delta P_{L2} \\ \Delta P_{PV} \\ \Delta F_1 \end{bmatrix} \quad (2)$$

$$y = [B_2 \ 0 \ 0 \ 0 \ 0 \ -1] \begin{bmatrix} \Delta F_2 \\ \Delta P_{DEG2} \\ \Delta X_{s2} \\ \Delta P_{BESS} \\ \Delta P_{ac} \end{bmatrix}$$

### IV. Designing a proposed controller for a two-area microgrid:

#### A. MPC

The utilization of MPC has been observed across a wide range of industries, including the chemical processes, oil sector, and electromechanical systems. Fig. 2 illustrates the overall configuration of the MPC controller. As per the diagram, the MPC controller makes use of a system model to forecast and regulate its forthcoming behavior. Within this controller, the generation of a control signal is achieved by minimizing a cost function. The horizon's control signal values are determined to ensure that the system's future output aligns with the specified reference path. To accomplish this objective, the cost function is minimized, typically by considering the squared difference between the controlled variables and their desired values, along with the sum of the squared control signals.

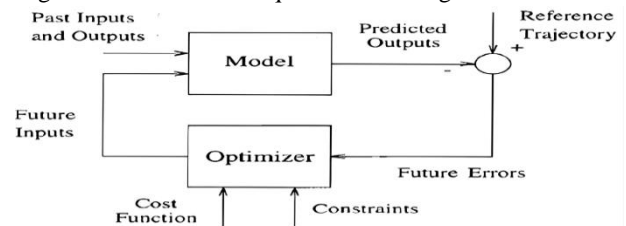


Fig. 2. Overall structure of the MPC

The cost function, represented by Equation (3), along with the constraints on the control signals (Equation (4)) and output signals (Equation (5)) are presented to manage and regulate the system.

$$J(N_1, N_2, N_u) = \min \sum_{j=N_1}^{N_2} ([y(k+j) - r(k+j)]^T W_y [y(k+j) - r(k+j)] + \sum_0^{N_u} ([u(k) - u(k-1)]^T W_u [u(k) - u(k-1)])) \quad (3)$$

$$u_{\min} \leq u(k) \leq u_{\max} \quad (4)$$

$$y_{\min} \leq y(k) \leq y_{\max} \quad (5)$$

In Equations (3) and (4),  $J(N_1, N_2, N_u)$  is the cost function which is to be minimized,  $N_1$  is the lower prediction horizon,  $N_2$  is the upper prediction horizon,  $N_u$  is the control horizon,  $y(k+j)$  is the output signal at  $k+j$ ,  $r(k+j)$  is reference output in control horizon at  $k+j$ ,  $u(k-1)$  is the calculated control signal at  $k-1$ , and  $W_y$ ,  $W_u$  are respectively the input weight matrix and the output weight matrix. The information depicted in Fig. 3 illustrates the sequential process of determining control signals and the corresponding calculations involved.

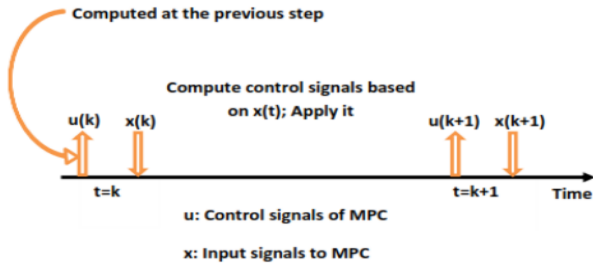


Fig. 3. The sequential process of determining control signals and the corresponding calculations

Variation in the generated power of the sources and load in each microgrid results in the variation of frequency and power of the connection line of the two microgrids. The power sources of a microgrid are categorized into two sections: controllable sources including DEG, BESS, and SMES; and b, uncontrollable sources including WTG and PV. When designing the MPC, variations of uncontrollable power sources are considered as predictable turbulence and load variation is considered as unpredictable turbulence. State-space equations for both controllers are formulated in Equation (6):

$$\begin{aligned} \dot{X}_i &= A_i X_i + B_i U_i + D_i W_i & i &= 1, 2 \\ Y_i &= C_i X_i \end{aligned} \quad (6)$$

In Equation (6),  $X_{i=1,2}$  is the vector of state variables for the first and second MPC,  $B_{i=1,2}$  is factor matrix of the first and the second MPC,  $U_{i=1,2}$  is the output control vector of the first and the second MPC,  $W_{i=1,2}$  is the turbulence vector

(uncontrollable input) of the first and the second MPC, and  $D$  is turbulence factor matrix for the first and the second MPC. Equations (7) and (8) are respectively complementary control errors of the first and second microgrid. With help of Equations (1) and (2) respectively, state-space equations for the MPC of the first and the second microgrid are written.

$$ACE_1 = \beta_1 \Delta F_1 + \Delta P_{tie} \quad (7)$$

$$ACE_2 = \beta_2 \Delta F_2 - \Delta P_{tie} \quad (8)$$

In Equations (7) and (8),  $ACE_1$  is the complementary control error of the first area,  $ACE_2$  is the complementary control error of the second area,  $\beta_1$ ,  $\beta_2$  are respectively bias frequency of the first and the second regions, and  $\Delta P_{tie}$  is power variations of the connection line. Based on the information provided in Fig. 4 of the proposed controller, the initial phase involves assessing and measuring variations in load, power resources, and microgrid frequency. Subsequently, the system's output (ACE) is predicted, and the appropriate controller signals are applied using a prescribed rule.

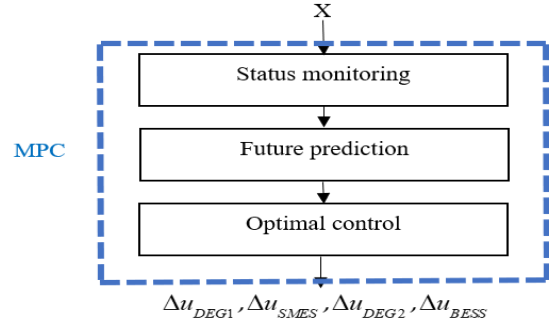


Fig. 4. The MPC controller

The behavior of the controller is governed by a set of equations, specifically Equation (9) to (14), which are explained in detail.

$$\begin{aligned} \min J &= \sum_{j=N_1}^{N_2} W_{y_i} (ACE_n(k+j))^2 + \\ &\sum_{i=1}^{N_u} W_{u_i} (\Delta u(k+j) - \Delta u(k+j-1))^2 \end{aligned} \quad (9)$$

$$\Delta u(k) = \Delta u(k-1) + \sum_{i=0}^{N_f} \delta_i ACE_n(k-i) \quad (10)$$

$$W_{y_i, \min} \leq W_{y_i} \leq W_{y_i, \max} \quad (11)$$

$$W_{u_i, \min} \leq W_{u_i} \leq W_{u_i, \max}$$

$$\begin{aligned} \Delta u &= \{\Delta u(k), \Delta u(k+1), \dots, \Delta u(k+N_u)\} \\ \Delta u &= [\Delta u_{DEG1}, \Delta u_{SMES}, \Delta u_{DEG2}, \Delta u_{BESS}] \end{aligned} \quad (12)$$

$$\begin{aligned} X(k+1) &= AX(k) + Bu(k) + DW(k) \\ Y(k) &= CX(k) \end{aligned} \quad (13)$$

$$P_{index} = \int_0^T t(|ACE_1| dt + \int_0^T |ACE_2|) dt \quad (14)$$

Equation (9) represents an objective function that has been designed to be quadratic. By minimizing this function, a set of control signals (described in Equation (12)) can be derived. Equation (10) describes how to calculate the  $\Delta u$  signal at each time step. The variable " $\delta_i$ " corresponds to the numerical coefficients that are determined through the solution of the optimization problem, specifically the minimization of the objective function "J". Equation (11) provides the specified ranges for the coefficients employed in the objective function. Equation (13) demonstrates the procedure for computing the state variables at any given time step. Equation (14) is derived during the calculations as an index, which serves as a comparative measure for evaluating different control methods in the simulation section.

### B. Optimizing weight parameters related to MPC controller using CRPSO algorithm

The PSO algorithm is a computational model and stochastic search technique inspired by swarm intelligence. It updates the position and velocity of each particle using Equations (15) and (16).

$$v_i^{k+1} = v_i^k + c_1 r_1 (P_{best} - x_i^k) + c_2 r_2 (g_{best} - x_i^k) \quad (15)$$

$$x_i^{k+1} = x_i^k + v_i^{k+1} \quad (16)$$

Equation (17) is utilized to update the velocity equations within the PSO algorithm, enhancing its overall search capability. Additionally, by incorporating a concept known as "craziness" into the algorithm, the position of the particle is updated using Equation (18), which is referred to as the CRPSO technique [31-34].

$$v_i^{k+1} = r_2 \text{sign}(r_3) v_i^k + (1 - r_2) c_1 r_1 (P_{best} - x_i^k) + (1 - r_2) c_2 (1 - r_1) (g_{best} - x_i^k) \\ \text{sign}(r_3) = \begin{cases} -1 & r_3 \leq 0.05 \\ 1 & r_3 > 0.05 \end{cases} \quad (17)$$

$$\left\{ \begin{array}{l} x_i^{k+1} = P_r(r_4) \text{sign}(r_4) v_i^{\text{craziness}} + v_i^{k+1} \\ P_r(r_4) = \begin{cases} 1 & r_4 \leq P_{craz} \\ 0 & r_4 > P_{craz} \end{cases} \\ \text{sign}(r_4) = \begin{cases} 1 & r_4 \leq 0.05 \\ -1 & r_4 > 0.05 \end{cases} \end{array} \right. \quad (18)$$

In this paper, the weight parameters of the MPC controller are considered to be the most influential adjustable parameter, significantly affecting the system response. As a result, the CRPSO algorithm is employed to optimize these weight parameters. The selection of the CRPSO algorithm is based on

its demonstrated effectiveness and efficiency in achieving optimal solutions quickly, surpassing the performance of other algorithms. Equation (19) represents the objective function used to fine-tune the weight parameters associated with the microgrid's LFC system in the MPC controller. The constraints for this optimization process are defined by Equation (11).

$$P_{index} = \min \int_0^T t(|ACE_1| dt + \int_0^T |ACE_2|) dt \quad (19)$$

The goal of optimization is to minimize the ITAE by adjusting the weight matrices  $W_{yi}$  and  $W_{ui}$ , which serve as input and output matrices, respectively. The following steps outline the process of optimizing the weight parameter of the MPC controller.

1. The optimization process begins with an initialization step where various parameters are set. This includes selecting a particle population size of 100 and specifying the maximum number of iterations as 100. Additionally, the values of  $c_1$  and  $c_2$  are set to 1.8 and 2.2, respectively, while the exploration rate ( $P_r$ ) is set to 0.28. Typically, the  $P_r$  value falls within the range of 0.4 to 0.9. Optimization algorithms involve two fundamental concepts: exploration and exploitation. Exploration refers to the generation of new solutions through random search, while exploitation involves refining and improving current solutions through local search. By increasing  $P_r$ ,  $c_1$ , and  $c_2$ , the emphasis is placed on exploration, whereas decreasing these values favors exploitation. Optimization algorithms are designed to initially have a high exploration rate and a low exploitation rate. As the process progresses, the exploration rate decreases while the exploitation rate increases. Therefore, it is crucial to consider this aspect during implementation, and the initial values of  $P_r$ ,  $c_1$ , and  $c_2$  are selected to be high and gradually decreased. These initial values are chosen to initiate the algorithm effectively.

2. Generate an initial population of particles randomly according to the  $\{W_{yi}, W_{ui}\} \in [0, 1]$ .

3. For every particle in the optimization process, the objective function is evaluated using Equation (19). This evaluation determines the fitness or performance of each particle. Based on the evaluation,  $P_{best}$  is determined for each particle, representing the best solution found by that particle so far. Additionally,  $g_{best}$  is determined for the entire group of particles, representing the best solution found among all particles in the population.

4. The velocity of the particles is calculated using Equations (17), and based on this velocity, the new positions of the particles are determined using Equation (18). In other words, the particles' movements are determined by their velocities, and their positions are updated accordingly.

5. Repeat steps (3) and (4) until the maximum number of iterations is reached.

6. Identify the particle that achieves the optimal solution.

In the MPC control method being proposed, the optimization problem described in Equation (19) needs to be solved at the start of each cycle, specifically at moment  $k$ , in order to calculate the  $X$  vector. The  $X$  vector are defined in Equations (1) and (2). In this method, the variables' vectors are updated only once, along with the forecast horizon  $N$ , which helps to significantly reduce the computational workload. These updated vectors are then optimized using the CRPSO.

The PSO algorithm involves defining the position and velocity variables for each particle. In this paper, both the position and velocity vectors are linear and have the same dimension as the decision variables in the  $X$  vector. These particles navigate the problem space with the aim of discovering the optimal solution. In the initial step, the position of a particle, denoted as variable  $X$ , is initialized along with the predicted values serving as model inputs. The timer counter  $k$  is set to zero to indicate the beginning of the optimization process. In the second step, the time step is incremented by  $k++$ . In the third step, the value of  $P_{index}$  ( $ACE_1+ACE_2$ ) is calculated. If  $P_{index}$  ( $ACE_1+ACE_2$ ) is not equal to zero, the process proceeds to the next step. In the fourth step, the particles and MPC control variables are updated. In the sixth step, if the number of time steps  $k$  reaches  $N$ , the process is terminated, and the objective function is evaluated using Equation (19) [31-33].

## V. Simulation

### A. Optimization of the problem

The weight parameters of MPC controllers have been optimized using three different algorithms: CRPSO, PSO, and GA. Initially, a change in the microgrid load of the first area was introduced, as shown in TABLE 1, with  $\Delta P_{L1}(pu)=0.05pu$  at  $t=0$ . The optimization process, as depicted in Fig. 5, consisted of 100 iterations for each algorithm. Among the three algorithms, CRPSO exhibited favorable results. It converged in the 23rd iteration, achieving an impressive objective function (ITAE) value of 0.0019. Comparatively, PSO reached convergence in the 82nd iteration with an objective function value of 0.0028, while GA converged in the 58th iteration, yielding an objective function value of 0.0029. Given its faster convergence and lower objective function value, CRPSO was selected to optimize the weight parameters associated with the MPC. The weight parameters obtained through CRPSO for the MPC are as follows:  $W_{y1}=0.5519$ ,  $W_{u2}=0.0461$ ,  $W_{y2}=0.5175$ , and  $W_{u1}=0.0772$ . These values were determined to enhance the performance of the MPC system.

### B. Different scenarios

The simulation was conducted under four distinct scenarios. In scenario (1), the focus was solely on load variations within the microgrid of the first area. Scenario (2) expanded the scope to include changes in both the load and the power output of the WTG associated with the first area's microgrid. Moving further, scenario (3) involved

simultaneous load fluctuations in the first microgrid and power variations in the distributed generation sources of the second microgrid. Notably, this scenario also accounted for the uncertainty in microgrid inertia within the first area.

Scenario (1):

In this scenario, the changes in the power of distributed production sources in both microgrids are not considered, and only the load changes in the first microgrid are considered. Based on Fig. 1 have been simulated. Changes in the load of the first microgrid as much as  $\Delta P_{L1}(pu)=0.05pu$  have occurred at the moment  $t=0$ . Figs 6, 7 and 8 respectively show the frequency changes of the first microgrid, the frequency changes of the second microgrid and the power changes of the communication line based on different controllers. The proposed controller (MPC(CRPSO)) was able to reduce the frequency deviations of the microgrid First, to minimize microgrid frequency deviations and power fluctuations of the communication line. The maximum frequency deviation of microgrid in area 1, the maximum frequency deviation of area 2 microgrid and the maximum deviation of power fluctuations between two microgrids have been improved by 20%, 25% and 42% by the proposed method. The settling time related to frequency deviation of microgrid in area 1 has been improved by 9% using the proposed controller. The settling time related to frequency deviation of area 2 microgrid has been improved by 13% using the proposed controller. Also, the settling time related to power power fluctuations between two microgrids has been improved by 7% using the proposed controller.

TABLE 1  
THE PARAMETERS OF THE COMBINED ALGORITHM AND MPC

parameter	value	parameter	value
$N_2(mpc_1)$	5	$T(mpc_{1,2})$	0.1
$N_u(mpc_{1,2})$	3	$N_2(mpc_2)$	5

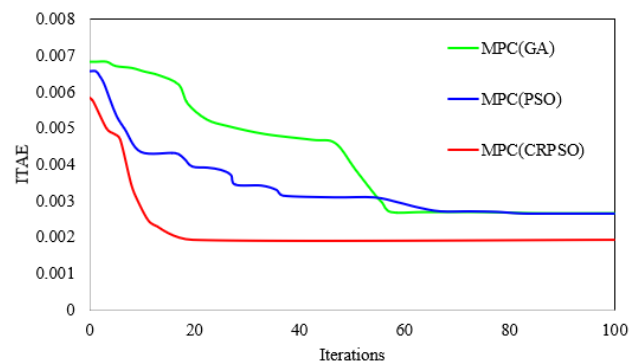


Fig. 5. The convergence of the different algorithms to solve the problem

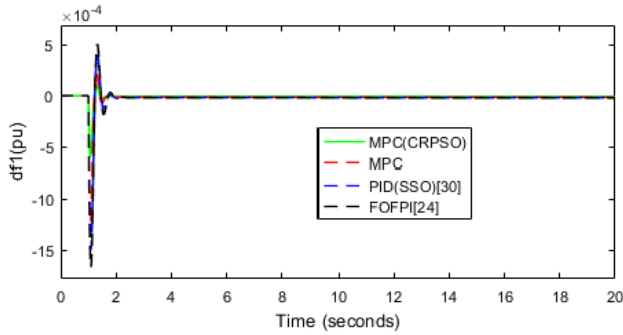


Fig. 6. The frequency changes of the first microgrid, scenario 1

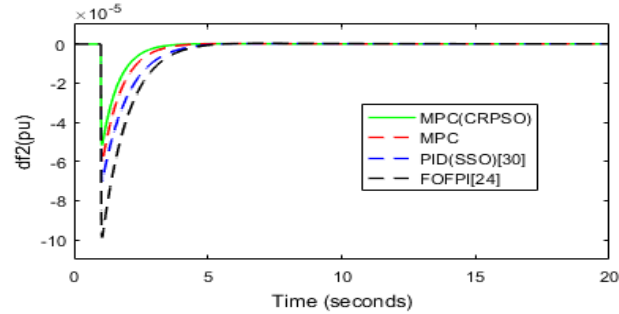


Fig. 7. The frequency changes of the second microgrid, scenario 1

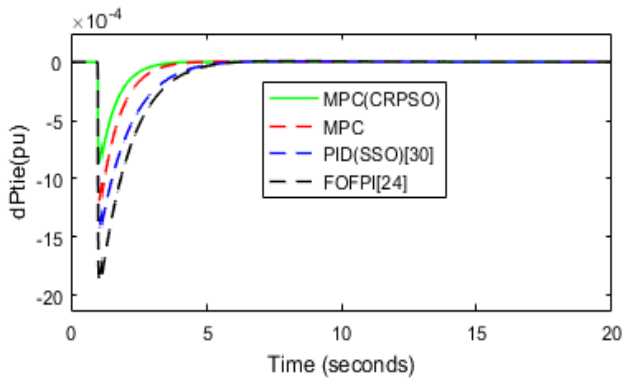


Fig. 8. The power changes of the communication line based on different controllers, scenario 1

Scenario (2):

In this scenario, the changes in the WTG and the load in the microgrid of the first area have happened. At  $t=0s$ , the load changes by the amount of  $\Delta P_{L1}(pu)=0.05pu$ , and at  $t=10s$ , the change in the speed of the WTG by the amount of  $\Delta V_{w1}=2(m/s)$ , and at  $t=15s$ , the change in the speed of the WTG by the amount of  $\Delta V_{w1}=-2(m/s)$  has occurred [30]. Figs 9, 10 and 11 respectively, the frequency changes of the first microgrid, the frequency changes of the second microgrid and the power changes of the communication line (system response to load changes) are shown based on different controllers. The proposed controller (MPC(CRPSO)) was able to reduce the microgrid frequency deviations First, to minimize microgrid frequency deviations and power fluctuations of the communication line. The maximum frequency deviation of microgrid in area 1, the maximum frequency deviation of area

2 microgrid and the maximum deviation of power fluctuations between two microgrids have been improved by 66%, 19% and 51% by the proposed method. The settling time related to frequency deviation of microgrid in area 1 has been improved by 19% using the proposed controller. The settling time related to frequency deviation of area 2 microgrid has been improved by 15% using the proposed controller. Also, the settling time related to power power fluctuations between two microgrids has been improved by 20% using the proposed controller.

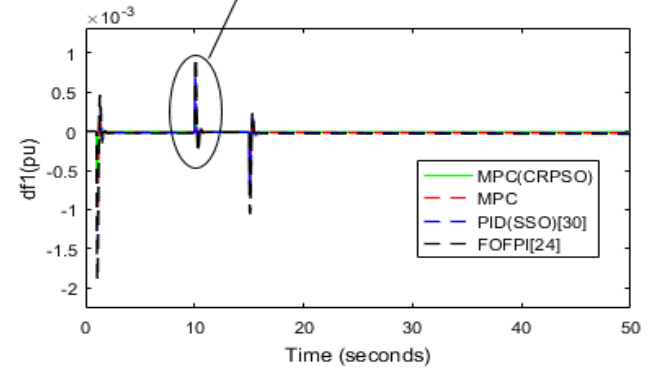
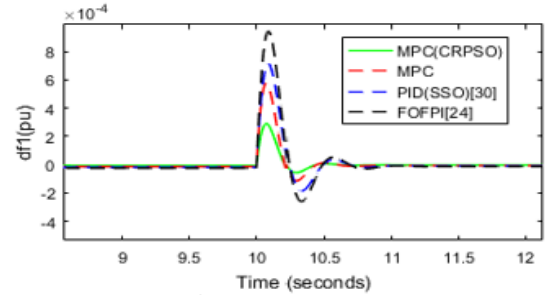


Fig. 9. The frequency changes of the first microgrid, scenario 2

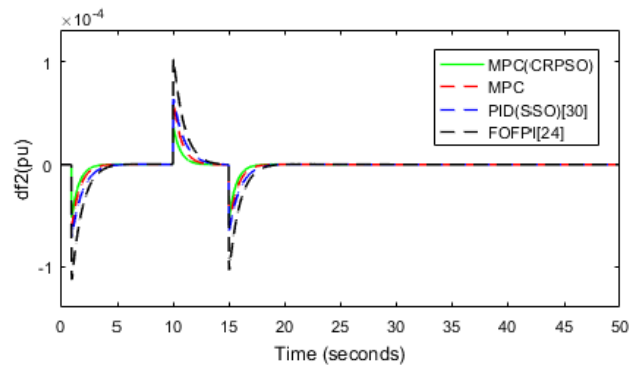


Fig. 10. The frequency variations for second microgrid, scenario 2



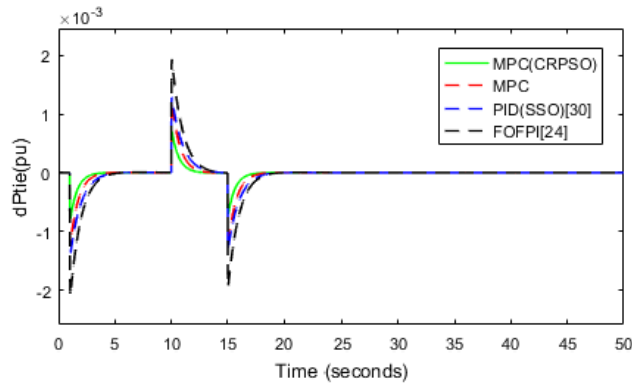


Fig. 11. The power changes of the communication line based on different controllers, scenario 2

### Scenario (3):

In this scenario, changes in PV power (second area) and load changes in the microgrid of the first area have occurred. Also, the uncertainty in the inertia parameter of the first microgrid ( $H=-10\%$ ) is considered. At  $t=0s$ , the load changes by the amount of  $\Delta P_{L1}(pu)=0.05pu$ , and at  $t=10s$ , the change in PV radiation by the amount of  $\Delta G_2=400(w/m^2)$ , and at  $t=15s$ , the change in PV radiation by the amount of  $\Delta G_2=-400(w/m^2)$ , Figs 12, 13 and 14 show the frequency changes of the first microgrid, the frequency changes of the second microgrid and the power changes of the communication line (system response to load changes) respectively. The proposed controller (MPC(CRPSO)) was able to reduce the microgrid frequency deviations. First, it minimizes the frequency deviations of the second microgrid and the fluctuations of the power of the communication line, and it is also resistant to the uncertainty related to the parameters of the two-area microgrid. The maximum frequency deviation of microgrid in area 1, the maximum frequency deviation of area 2 microgrid and the maximum deviation of power fluctuations between two microgrids have been improved by 59%, 24% and 42% by the proposed method. The settling time related to frequency deviation of microgrid in area 1 has been improved by 22% using the proposed controller. The settling time related to frequency deviation of area 2 microgrid has been improved by 8% using the proposed controller. Also, the settling time related to power power fluctuations between two microgrids has been improved by 9% using the proposed controller.

## VI. Conclusion

In this paper, the MPC whose weight parameters are used using the CRPSO is used for LFC in the two-area microgrid, as well as the number of controllers used for energy storage sources in the microgrid using the controller method. The proposal is reduced (less complexity). According to the results

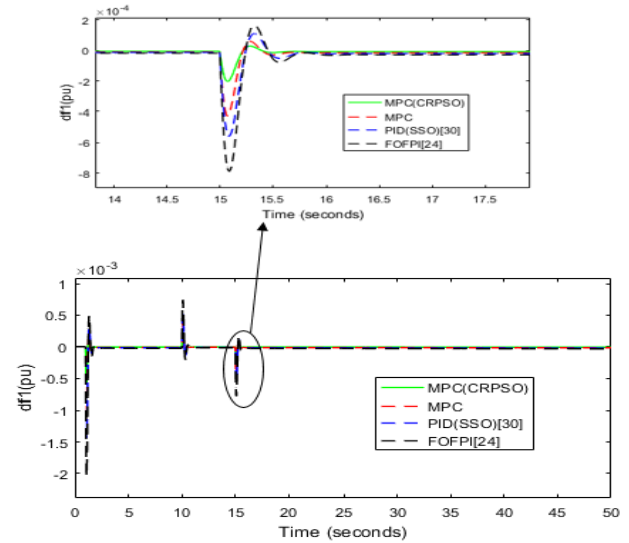


Fig. 12. The frequency changes of the first microgrid, scenario 3

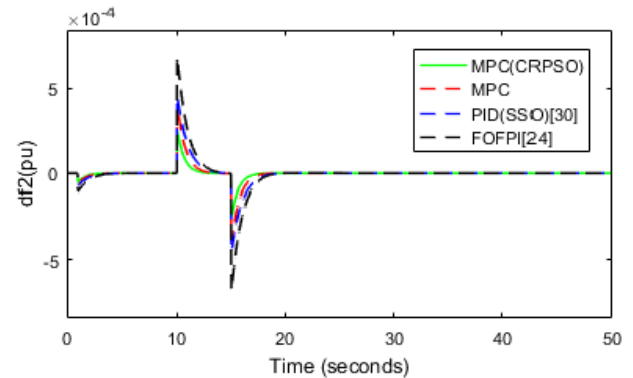


Fig. 13. The frequency variations for second microgrid, scenario 3

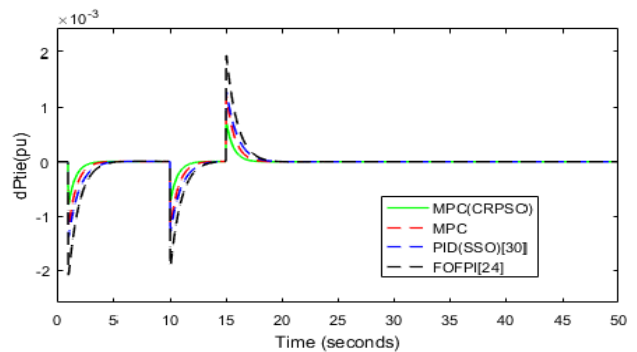


Fig. 14. The power changes of the communication line based on different controllers, scenario 3

of the proposed controller and its comparison with different controllers, the effectiveness of the proposed method in reducing the use of fewer controllers (less complexity) has been shown, as well as the optimal performance of the proposed controller in terms of response speed and reducing overshoot and overshoot. It has been shown. The proposed

method has also been able to be resistant to disturbances and uncertainty related to two-area microgrid parameters.

## REFERENCES

- [1] M. Jami, "Virtual Inertia Control and Small-Signal Stability Analysis of Electric Vehicle," *International Journal of Industrial Electronics Control and Optimization*, 2023.
- [2] M. Safdari, M. R. Alizadeh Pahlavani, A. Dehestani Kolagar, "Model Predictive Voltage Balance Control of Single-Phase Half-Bridge Active Front End Rectifier," *International Journal of Industrial Electronics Control and Optimization*, 2023.
- [3] F. Amiri, M. H. Moradi, "Improvement of Frequency stability in the power system considering wind turbine and time delay," *Journal of Renewable Energy and Environment*, Vol. 10. No. 1, pp. 9-18, 2023.
- [4] M. Shahbazi, F. Amiri, (2019, December). Designing a Neuro-Fuzzy controller with CRPSO and RLSE algorithms to control voltage and frequency in an isolated microgrid. In *2019 International Power System Conference (PSC)* (pp. 588-594). IEEE.
- [5] F. Amiri, A. Hatami, "A model predictive control method for load-frequency control in islanded microgrids," *Computational Intelligence in Electrical Engineering*, Vol. 8, No. 1, pp. 9-24, 2017.
- [6] F. Amiri, M. Moradi, "Designing a new robust control for virtual inertia control in the microgrid with regard to virtual damping," *Journal of Electrical and Computer Engineering Innovations (JECEI)*, Vol. 8, No. 1, pp. 53-70, 2019.
- [7] H. Gu, T. Banki, A. Soleymani, "Robust Frequency Control of Additive Manufacturing Based Microgrid Considering Delayed Fuel Cell Dynamics," *Journal of New Materials for Electrochemical Systems*, Vol. 26, No. 4, 2023.
- [8] F. Amiri, A. Hatami, "Load Frequency Control Via Adaptive Fuzzy PID Controller In An Isolated Microgrid", In *32nd international power system conference*, 2017.
- [9] F. Amiri, M. Eskandari, M. H. Moradi, "Improved Load Frequency Control in Power Systems Hosting Wind Turbines by an Augmented Fractional Order PID Controller Optimized by the Powerful Owl Search Algorithm," *Algorithms*, Vol. 16, No. 12, pp. 539., 2023.
- [10] D. Murugesan, K. Jagatheesan, P. Shah, R. Sekhar, "Fractional order PIAD $\mu$  controller for microgrid power system using cohort intelligence optimization," *Results in Control and Optimization*, Vol. 11, pp. 100218, 2023.
- [11] K. Singh, M. Dahiya, A. Grover, R. Adlakha, M. Amir, "An effective cascade control strategy for frequency regulation of renewable energy based hybrid power system with energy storage system," *Journal of Energy Storage*, Vol. 68, pp. 107804, 2023.
- [12] H. A. Muqeet, R. Liaqat, M. Jamil, A. A. Khan, "A State-of-the-Art Review of Smart Energy Systems and Their Management in a Smart Grid Environment," *Energies*, Vol. 16, No. 1, pp. 472, 2023.
- [13] R. H. Kumar, S. Ushakumari, "Biogeography based tuning of PID controllers for Load Frequency Control in microgrid," In *2014 International Conference on Circuits, Power and Computing Technologies [ICCPCT-2014]* (pp. 797-802). IEEE, 2014.
- [14] G. Shankar, V. Mukherjee, "Load frequency control of an autonomous hybrid power system by quasi-oppositional harmony search algorithm," *International Journal of Electrical Power & Energy Systems*, Vol. 78, 715-734, 2016.
- [15] R. Mandal, K. Chatterjee, "Application and optimization of a robust fractional-order FOPI-FOPID automatic generation controller for a multiarea interconnected hybrid power system," In *Fractional Order Systems and Applications in Engineering* (pp. 175-197). Academic Press, 2023.
- [16] I. Pan, S. Das, "Fractional order fuzzy control of hybrid power system with renewable generation using chaotic PSO," *ISA transactions*, Vol. 62, pp. 19-29, 2016.
- [17] H. Shayeghi, I. F. Davoudkhani, N. Bizon, "Robust self-adaptive fuzzy controller for load-frequency control of islanded airport microgrids considering electric aircraft energy storage and demand response," *IET Renewable Power Generation*, 2024.
- [18] H. B. CH, C. Dhanamjayulu, I. Kamwa, S. M. Muyeen, "A novel on intelligent energy control strategy for micro grids with renewables and EVs," *Energy Strategy Reviews*, Vol. 52, pp. 101306, 2024.
- [19] H. Bevrani, F. Habibi, P. Babahajyani, M. Watanabe, Mitani, Y., "Intelligent frequency control in an AC microgrid: Online PSO-based fuzzy tuning appCRPSOch," *IEEE transactions on smart grid*, Vol. 3, No. 4, pp. 1935-1944, 2012.
- [20] M. R. Khalghani, M. H. Khooban, E. Mahboubi-Moghaddam, N. Vafamand, M. Goodarzi, "A self-tuning load frequency control strategy for microgrids: Human brain emotional learning," *International Journal of Electrical Power & Energy Systems*, Vol. 75, pp. 311-319, 2016.
- [21] S. K. Tripathi, V. P. Singh, Pandey, "Robust load frequency control of interconnected power system in smart grid," *IETE Journal of Research*", Vol. 69, No. 8, pp. 5351-5363, 2023.
- [22] H. Bevrani, M. R. Feizi, S. Atae, "Robust Frequency Control in an Islanded Microgrid:  $\{H\}_{\infty}$  and  $\mu$ -Synthesis AppCRPSOches," *IEEE transactions on smart grid*, Vol. 7, No. 2, pp. 706-717, 2015.
- [23] F. Amiri, A. Hatami, "Load frequency control for two-area hybrid microgrids using model predictive control optimized by grey wolf-pattern search algorithm," *Soft Computing*, pp. 1-17, 2023.
- [24] C. Mu, A. Naderipour, Z. Abdul-Malek, I. F. Davoodkhani, H. Kamyab, R. R. Ali, "Load-frequency control in an islanded microgrid PV/WT/FC/ESS using an optimal self-tuning fractional-order fuzzy controller," *Environmental Science and Pollution Research*, Vol. 30, No. 28, pp. 71677-71688, 2023.
- [25] P. Jampeethong, S. Khomfoi, "Coordinated Control of Electric Vehicles and Renewable Energy Sources for Frequency Regulation in Microgrids," *IEEE Access*, Vol. 8, pp. 141967-141976, 2020.
- [26] F. Amiri, M. H. Moradi, "Coordinated Control of LFC and SMES in the Power System Using a New Robust Controller," *Iranian Journal of Electrical and Electronic Engineering*, pp. 1912-1912, 2021.
- [27] F. Amiri, M. H. Moradi, "Designing a Fractional Order PID Controller for a Two-Area Micro-Grid under Uncertainty of Parameters," *Iranian journal of energy*, Vol. 20, No. 4, pp. 49-78, 2018.
- [28] V. P. Singh, N. Kishor, P. Samuel, "Communication time delay estimation for load frequency control in two-area

- power system," Ad Hoc Networks, Vol. 41, pp. 69-85, 2016.
- [29] F. Tedesco, A. Casavola, "Fault-tolerant distributed load/frequency coordination strategies for multi-area power microgrids," IFAC-PapersOnLine, Vol. 48, No. 21, pp. 54-59, 2015.
- [30] A. A. El-Fergany, M. A. El-Hameed, "Efficient frequency controllers for autonomous two-area two-area microgrid system using social-spider optimiser," IET Generation, Transmission & Distribution, Vol. 11, No. 3, pp. 637-648, 2017.
- [31] A. R. Moazzeni, E. Khamehchi, "Craziness based Particle Swarm Optimization (CRPSO): A new metaheuristic method for drilling optimization solutions," Journal of Petroleum Science and Engineering, Vol. 195, pp. 107512, 2020.
- [32] I. V. Pustokhina, D. A. Pustokhin, P. T. Nguyen, M. Elhoseny, K. Shankar, "Multi-objective Craziness based Particle Swarm Optimization with WELM model for customer churn prediction in telecommunication sector," Complex & Intelligent Systems, pp. 1-13, 2021.
- [33] S. Kumar, R. P. Mahapatra, "Design of multi-warehouse inventory model for an optimal replenishment policy using a Craziness based Particle Swarm Optimization," *Knowledge-Based Systems*, Vol. 231, 107406, 2021.
- [34] F. Amiri, M. H. Moradi, "A new control strategy for controlling isolated microgrid," Engineering and Energy Management, Vol. 10, No. 4, pp. 60-73, 2023.

---

Particle Swarm Optimization (PSO)  
 Biogeography-based(BIO)  
 Quasi-oppositional harmony (QOH)  
 Fractional order(FO)  
 Human brain emotional learning(HBEL)  
 Social-spider optimizer (SSO)  
 Wind Turbine Generator (WTG)

Diesel Engine Generator1 (DEG1)  
 Super Magnetic Energy Storage(SMES)  
 Diesel Engine Generator2 (DEG2)  
 Photo voltaic (PV)  
 Battery Energy Storage System(BESS)  
 Maximum Power Point Tracker(MPPT)  
 Model Predictive Controller(MPC)  
 Harmony search algorithm (HSA)

---



**Farhad Amiri** was born in Ilam. He received his MSc and PhD degrees in electrical engineering in 2017 and 2022, respectively, from Bu-Ali Sina University. He also received his post-doctoral (Electrical engineering) in 2024 from the National Elites Foundation of Iran. His research interests include dynamic and transient performance of power system, control, Microgrid and renewable energy.



**Mohammad Hassan Moradi** was born in Nowshahr, Mazandaran, Iran. He obtained his B.Sc., M.Sc. and PhD from Sharif University of Technology, Tarbiat Modares University and Strathclyde University in Glasgow, Scotland in 1991 1993 and 2002 respectively. His research interests include New and Green Energy, Microgrid Modeling and Control, DG Location and Sizing in Power System, photovoltaic systems and power electronics, Combined Heat and Power Plant, Power Quality, Supervisory Control, Fuzzy Control.